Acta Crystallographica Section D
**Biological Crystallography**
ISSN 0907-4449

# A nanovolume crystallization robot that creates its crystallization screens on-the-fly

**Bart Hazes* and Luke Price**

University of Alberta, Canada

Correspondence e-mail: bart.hazes@ualberta.ca

Received 4 May 2005
Accepted 1 June 2005

Protein crystallization generally consists of an initial screen followed by optimization of promising conditions. Whereas the initial screen typically uses a standard set of pre-made crystallization cocktails, optimization requires new cocktails with small perturbations of the original composition. Highly parallel synchronous crystallization robots are ideal for initial screening, but they depend on pre-made crystallization cocktails. Asynchronous crystallization robots can create crystallization cocktails from stock solutions, but in practice this ability is rarely exploited. Instead, large-scale operations typically use a general liquid-handling robot to create optimization screens, whereas academics mostly rely on manual optimization. Here, the use of an asynchronous crystallization robot to create customized crystallization cocktails and set up nanovolume crystallization experiments without a compromise in speed or drop quality is described. This approach avoids the complex integration of hardware, software and dataflow between two robots and saves cost and space. As a proof of principle, a commercial crystal screen has been reproduced with the robot and shows that results are virtually identical to using the actual commercial screen.

## 1. Introduction

In our pursuit to understand life, the field of molecular biology plays a special role as it studies life at its most basic level. Proteins are particularly important and many biotechnology applications and diseases can be understood by studying protein function at the molecular level (Machius, 2003). From an applied interest, the ultimate goal is therefore to reach a state where we can become active manipulators of protein function through direct protein engineering or the design of compounds that inhibit or modify protein function (Bott & Boelens, 1999; Blundell & Patel, 2004). The determination of three-dimensional atomic models of proteins is key to reaching this goal because the function of a protein results directly from the spatial arrangement of its atoms. Protein crystallography and nuclear magnetic resonance spectroscopy (NMR) are the main techniques for protein structure determination (Montelione *et al.*, 2000), but for large proteins and applications where high precision is required protein crystallography remains the method of choice.

The commercial interest in structural biology and the desire to complement the explosion of protein sequences from genome-sequencing projects with structural models created a demand for high-throughput protein crystallography in the late 1990s (Gaasterland, 1998; Dry *et al.*, 2000; Russell & Eggleston, 2000). In the preceding years, critical advances in

key steps of the structure-determination process set the stage for automation (Hendrickson, 2000) and, with significant capital influx from the pharmaceutical industry and government funding of large-scale structural genomics projects, rapid progress has been made. Cryo-crystallography (Garman, 2003; Pflugrath, 2004), third-generation synchrotrons (Hendrickson, 2000) and automated crystal mounting (Snell *et al.*, 2004; Pflugrath, 2004) have revolutionized diffraction data collection and the use of anomalous dispersion (Hendrickson *et al.*, 1989) combined with selenomethionine-substituted protein samples has provided a standard route to experimental phase determination (Hendrickson *et al.*, 1990). A second revolution has taken place in the downstream computational aspects of structure determination, where increasingly sophisticated software exploits the abundant computer power (Terwilliger, 2003; Potterton *et al.*, 2003; Cohen *et al.*, 2004; Adams *et al.*, 2004). Today, when good experimental data have been obtained, structure solution, refinement and validation can be carried out in a time frame of hours to days with little user intervention. In contrast, although considerable resources have been directed to protein production and crystallization, these upstream stages of the protein crystallography pipeline have seen much less progress and have become the limiting factors to overall throughput (Chayen, 2003; DeLucas *et al.*, 2005).

Protein crystallography requires that a highly purified protein sample be exposed to physicochemical conditions that stimulate nucleation and growth of single crystals of adequate size. Finding these conditions is a major challenge, as it depends on many poorly understood parameters, including the choice of crystallization method, temperature and the combination of precipitant, buffer and additives that define the crystallization cocktail. A unique set of crystallization conditions has to be worked out for each new protein and a common approach is to use a two-step procedure consisting of a broad initial screen followed by optimization of promising conditions. If no prior knowledge is available, the initial screen can sample a standard set of conditions and a common approach uses sparse-matrix sampling, where a set of screen conditions is selected based on past performance for other proteins (Jancarik & Kim, 1991). Many commercial screens are based on this principle and their pre-made solutions make it easy to set up the initial crystallization screen. However, when prior knowledge is available to customize the initial screen or when promising conditions need to be optimized, new crystallization cocktails must be created. In a low-throughput environment this is typically carried out manually, but automation is required to implement a thorough and systematic optimization protocol as part of a large-scale crystallization operation (Chayen & Saridakis, 2002; Chayen, 2003).

The repetitive nature of crystallization-experiment setup is well suited to automation and dedicated crystallization robots are commercially available. In addition to their ability to create experiments at a high rate and high density, several robots also miniaturize sample volumes and thereby reduce the amount of protein that needs to be produced (Hosfield *et al.*, 2003; Stock *et al.*, 2005). This latter feature is extremely important as it reduces the protein-production challenge. Unfortunately, nanovolume crystallization robots have so far not been widely used to create the crystallization screens and thus rely on pre-made solutions. For synchronous robots, where all dispense units operate in concert, this is an inherent limitation of the design. Examples are the Hummingbird (Genomic Solutions) and Hydra+1 (Robbins Scientific; Krupka *et al.*, 2002) robots. In contrast, the Honeybee (Genomic Solutions) and Screenmaker (Innovadyne Technologies Inc) are asynchronous robots, where each dispense unit operates independently. Such robots can in principle create custom-defined crystallization cocktails from stock solutions, but realising this in practice has been difficult. Instead, a general liquid-handling robot is often used to create the screen solutions, which are then fed into the crystallization robot for experiment setup (Rupp *et al.*, 2002; Stock *et al.*, 2005; DeLucas *et al.*, 2005). However, the expertise required to integrate hardware, software and dataflow between two robots and the extra operation cost, maintenance and space needed for a second robot are not always available, especially in academic environments. To provide access to the most advanced crystallization robot technology in an academic setting, we have developed software that enables a single asynchronous crystallization robot to create customized crystallization cocktails and set up nanovolume crystallization experiments without a compromise in speed or drop quality. The same system can also still set up screens from pre-made solutions with ease.

## 2. Automation implementation

### 2.1. Robot hardware design

**2.1.1. Dispense technology**. We have designed our robot based on the SynQuad non-contact dispense technology (Genomic Solutions), as its inherent properties closely match the needs of our application. Because it is important to understand the underlying technology, we will describe it in some detail and highlight key features that affect its use for screen creation and crystallization-drop setup. Innovadyne uses a related technology that may also be suitable. Fig. 1 shows the basic features of SynQuad technology.

The SynQuad technology uses a high-precision syringe to define dispense volumes and a solenoid valve to control the timing and speed of reagent dispense. The liquid volume that enters the reagent tubing for each dispense is fixed and set by the syringe. In contrast, the actual dispensed volume depends on the pressure in the reagent tubing and the open time of the solenoid valve. Initially, the pressure is low and more liquid enters the reagent tubing than is dispensed; this builds up pressure in the reagent tubing until a steady state is reached where the dispensed volume equals the set volume of the syringe. A series of pre-pressurization dispenses is used to reach the steady-state pressure, after which accurate volumetric dispensing is achieved independent of variations in viscosity or other properties. This is the basis for accurate

nanovolume dispensing and minimum dispense volumes as low as 20 nl have been reported (Hosfield *et al.*, 2003), although 50–100 nl are more routinely used to create crystallization drops (Hosfield *et al.*, 2003; Sulzenbacher *et al.*, 2002; Stock *et al.*, 2005).

The solenoid open time also controls dispense velocity, as shorter open times result in a higher pressure, which causes the reagent to be ejected at higher speed. With sufficient pressure, even viscous solutions are cleanly discharged from the nozzle, leading to non-contact dispensing. With some effort, 100 nl droplets containing up to 30% PEG 8K can be dispensed with this technology. Another important benefit of the high dispense velocity is that the kinetic energy of the droplets is sufficient to cause mixing on impact. The combination of non-contact dispensing and impact-based mixing is critical to our application, as it allows us to create the crystallization cocktail without contamination of the dispense tips. An important challenge of our approach is that the dispense of crystallization cocktails and the crystallization drop require volumes that differ by almost three orders of magnitude: 1–50 µl for the former and ∼100 nl for the latter. As described, SynQuad is inherently capable of dispensing very low volumes, but the maximum single-drop dispense volume is 1–4 µl. However, larger volumes are easily accommodated by dispensing multiple drops or alternatively by locking the solenoid valve in the open position so that the syringe takes direct control of liquid delivery. In conclusion, SynQuad technology is fully capable of creating crystallization cocktails and setting up crystallization drops. However, filling each reservoir of a standard 96-well crystallization plate with 50 µl of crystallization cocktail requires that 4.8 ml of a reasonable number of distinct reagents can be dispensed. The available number of dispense units and the dispense mode have to be chosen to match this requirement.

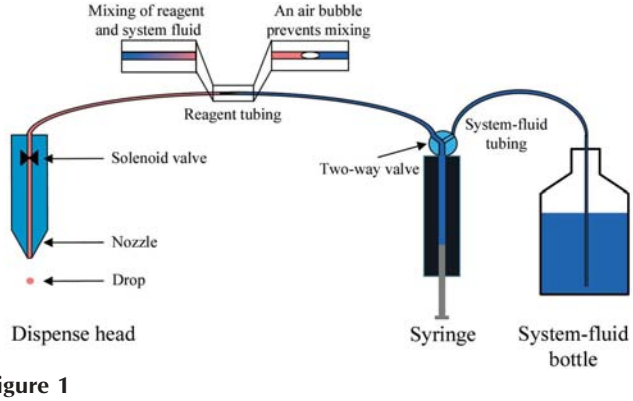


**Figure 1**
SynQuad dispense technology. A motor-driven high-precision syringe is coupled to a two-way valve. Repeated aspiration from the system-fluid bottle and dispense *via* the dispense head is used to clean the system or to dispense in unidirectional mode (see §2.1.2). In the aspirate-dispense mode, the nozzle is submersed in a reagent and, with the solenoid valve open, the syringe then aspirates reagent into the dispense head and reagent tubing. Without precautions, turbulent mixing occurs on the interface between reagent and system fluid, an air bubble can prevent this (see insets). During SynQuad dispensing, the solenoid valve opens very briefly and the dispensed volume and speed of the reagent depend on the pressure in the reagent tubing. After a series of pre-pressurization dispenses, the volume dispensed by the syringe becomes the same as the volume ejected from the dispense head, yielding a steady state (see main text for details).

**2.1.2. Dispense modes**. SynQuad dispensing can use two distinct dispense modes. In one mode, reagents are supplied as the system fluid and the reagent is pumped in a unidirectional manner from the system-fluid bottle through the system tubing, syringe and reagent tubing. A major advantage is that the volume that can be dispensed in this mode is virtually unlimited. The main disadvantage is that each dispense unit can dispense only a single reagent and the number of dispense heads must thus equal or exceed the number of reagents needed by the application. In the alternative mode, the aspirate-dispense mode, reagent is first aspirated through the dispense head into the reagent tubing before being delivered at the desired location (depicted in Fig. 1). This provides access to a virtually unlimited number of reagents, but the maximum volume that can be delivered in a single pass is limited to the internal volume of the reagent tubing. Furthermore, if the aspirated reagent is in contact with the system fluid then turbulent mixing at the liquid interface will lead to dilution (see Fig. 1, left inset). As a consequence, only ∼50% of the aspirated volume can be dispensed; the

**Figure 2**
Image of the Honeybee robot (Genomic Solutions) with the syringes on top of the humidity-controlled cabinet that holds the plate deck, sample and wash stations and the dispense heads. An enlargement of the 32 reagent dispense heads and one extra protein dispense head is shown in the bottom right corner.

remainder will be diluted by mixing. To avoid this, one can simply separate the reagent from the system fluid by an air bubble (Fig. 1, right inset). Because the air bubble should not enter the syringe, the maximum dispense volume is set by the volume of the reagent tubing. In our system the reagent tubing holds ~300 µl and we aspirate up to 250 µl, which matches the volume of our syringes. Longer tubing can accommodate higher volumes, but may reduce the accuracy of nanovolume dispensing.

**2.1.3. Number of dispense units**. We have equipped our system with 32 reagent-dispense units using the Honeybee 'ProSys' robotics platform from Genomic Solutions (Fig. 2). This number is a compromise between cost and complexity of the system and the practical needs for a typical crystallization screen. Crystal Screen I (Hampton Research) contains 29 distinct reagents and our robot can recreate this screen and others of similar complexity from individual stock solutions (see below). Our 32 syringes can also dispense a combined 8 ml (32 × 250 µl) of reagent solutions, which exceeds the 4.8 ml needed to fill 96 reservoirs with 50 µl each. Dispense volume is further increased by a two-pass procedure where water is added to each well in a rapid first pass, followed by addition of reagents in the second pass. Since the reagent dispense pass takes less than 3 min for a 96-well plate, it is easy to add multiple passes for robots with fewer dispense units or for more complex screens.

### 2.2. Robot software design

**2.2.1. Combinatorial dispense algorithm**. The basic goal for our software is to allow a user or expert system to define a crystallization screen in which each reservoir of a crystallization plate receives any desired combination of reagents selected from 32 stock solutions. Rather than calculating a complex set of screen-specific robot motions, we have adopted a simple procedure in which the dispense head is scanned over the crystallization plate so that each dispense unit visits each reservoir well of the plate (Fig. 3). The computational problem is thus reduced to timing the dispenses so that a dispense is triggered only if a dispense unit is over a reservoir that requires that reagent. The implementation is divided into a dispense-timing program named *RoboDrop* (see §2.2.2) and a motion program, defined using the robot control software, that drives the scanning motion of the dispense head. At each of the 225 steps of the scan the dispense information is read from a text file created by *RoboDrop* (225 lines with 32 numbers per line describing the dispense volume for each dispense unit). Since multiple dispense units can fire simultaneously at each step, the time per step depends only on the largest dispense volume of each step. The time for a complete plate fill thus depends on the number of steps but not on the complexity of the crystallization cocktails. In practice, the entire scan takes less than 3 min.

**2.2.2. Screen definition interface**. We have created a GUI-based program (*RoboDrop*) to hide the complexities of creating the text file that defines the dispense volumes. A picture of the interface is shown in Fig. 4. In the top panel the user defines the 32 stock solutions by typing or by reading from a previously saved file. The user then selects one of the 32 stock solutions (its background colour will change to orange) and uses the control panel on the left to indicate if it is to be used as a precipitant, buffer or additive. A left mouse button click on a well in the destination plate (lower right panel) will add that stock solution to the well, with precipitant, buffer and additive appearing on lines 1, 2 and 3, respectively. Similarly, a right mouse-button click sets the percentage of the total reservoir volume for that stock solution. By clicking on the column, row and plate identifiers along the top, left and top-left corner of the destination plate, respectively, definitions can be added to entire columns, rows or the whole plate. As the destination plate is filled, the software ensures that reagent percentages for a single well never exceed 100%. Similarly, if the user sets the total reservoir volume in the control panel then the software issues a warning if the requested reagent volume for a single stock solution exceeds 240 µl, the maximum total dispense volume per dispense unit. For screens that need more of a particular reagent, we simply aspirate that reagent into two or more dispense units (see E1 and H2 in the top panel of Fig. 4). As a final feature, the user can decrease the precipitant concentration in all wells through the 'strength' parameter in the control panel. In this way a

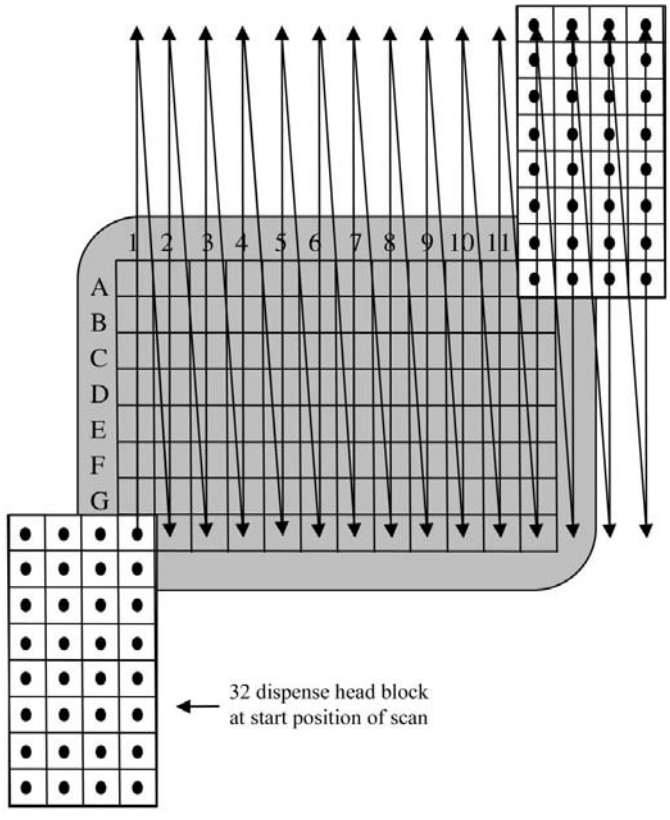


**Figure 3**
Schematic diagram of the scanning motion during combinatorial dispensing. The dispense heads start at the lower left with the top-right dispense head over well H1 of a 96-well plate. The arrows indicate the trajectory of this dispense head which, after 225 steps, ends up at the top-right corner position, as indicated. At each step of the scan, zero or more dispense heads may simultaneously discharge reagents.

standard screen can be adjusted for less soluble proteins. When a screen definition is completed, the program computes how much water needs to be added to each well and then a text file with all dispense instructions for the robot is written. The screen definition can also be saved for future re-use, for reading into a LIMS or other database or to annotate images of the crystallization experiments. *RoboDrop* is written in the Python programming language and can thus be run by end users on virtually any computer (Windows PC, Macintosh, Unix/Linux). To use the robot, the users simply provide their protein sample, stock solution plate and the text file made by *RoboDrop*.

### 2.3. Proof of concept

To demonstrate the value of our system in a real-life exercise we have used the *RoboDrop* program to recreate 48 conditions of Crystal Screen 1 (Hampton Research) and the same 48 conditions of the 'Lite' version of the screen (identical to Crystal Screen 1 but with half the precipitant concentration). The screen definition is shown in Fig. 4. The stock solutions were provided in the first four columns of a 96-well plate. As test proteins we used hen egg-white lysozyme (Sigma, 50 mg ml$^{-1}$ in 0.1 *M* sodium acetate pH 4.8), *Thaumatococcus daniellii* thaumatin (Sigma, 50 mg ml$^{-1}$ in water) and glucose isomerase (Hampton Research, 26 mg ml$^{-1}$ in water). Total plate-setup time from initial tip washing to completion of the third protein dispense took 20 min, which is identical to the time taken to set up a plate using pre-made commercial solutions. Fig. 5 shows the crystallization results for the combinatorial and commercial screens, respectively. The strong correlation in crystallization success between the two screens on all three test proteins attests to the accuracy of the combinatorial screens. We have also used food dyes dissolved in solutions of increasing viscosity to visually confirm proper mixing when two 25 µl volumes were dispensed on top of each other (results not shown).

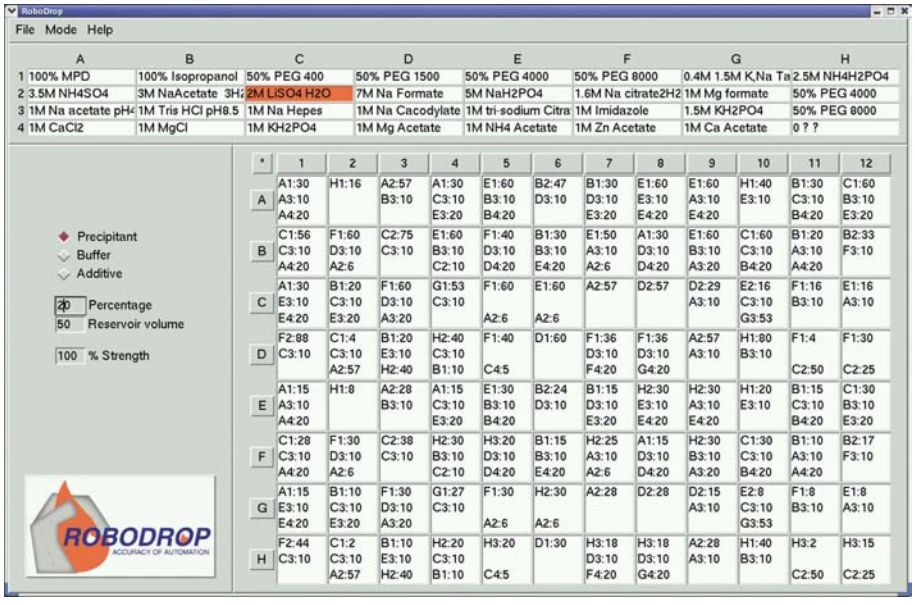


**Figure 4**
The *RoboDrop* graphical user interface. The top panel (source-plate panel) defines the stock solution chemistries. Input can be any text string and it is currently simply used as a label. The bottom right panel (destination plate) represents the 96 chambers of the crystallization plate. Each cell currently has three lines that, from top to bottom, define the precipitant, buffer and additive composition of the reservoir solution. Empty lines indicate that no reagent of that type is needed. Each line contains a two-character identifier that corresponds to the source-plate well, separated by a colon from the desired volume, given as a percentage of the total reservoir volume. The bottom left panel (control panel) allows the user to set the class (precipitant, buffer, additive) and percentage for the 'selected reagent' (highlighted in orange in the source plate panel). The 'Drop volume' field sets the total volume of reservoir solution to prepare and the '% Strength' field allows the user to lower the precipitant concentration of all wells without affecting the buffer and additive composition.

## 3. Discussion

Our goal is to create a regional facility that brings the benefits from high-throughput crystallization to an academic user base. Although no single academic laboratory can claim to need the enormous throughput provided by the crystallization robot described above, crystallization robots provide far more than a quantitative scale-up. Foremost is the miniaturization that reduces protein consumption fivefold to tenfold. Secondly, time pressures and human nature often result in crystallization screens that are not as thorough as they could be. In addition, approaches where multiple mutants, orthologs or truncation variants of the target protein are pursued in parallel are often beyond the scope of academic research (Grimm *et al.*, 2000; Derewenda, 2004). By reducing the labor cost, crystallization robots stimulate the use of more thorough and aggressive crystallization approaches, which increase the probability of success, reduce time to completion and allow more challenging problems to be undertaken. Thoroughness also extends to the optimization of promising crystallization conditions. Optimization has been recognized as a critical component of crystallization (Chayen & Saridakis, 2002; Chayen, 2003), but without access to a crystallization robot typically only one or a few conditions are optimized. This is unfortunate, as it is hard to predict which condition will give the best result. In addition, optimizing multiple conditions may yield multiple crystal forms that can benefit structure determination. The best diffracting crystal is also not always the one that is most suitable for phasing or for future protein–inhibitor complex studies. Finally, an underappreciated aspect of crystallization robots is that they enable a whole new group of users to become involved in protein crystallization. The combination of reduced protein consumption and hands-off crystallization experiment setup has started to

mobilize colleagues that had not previously dared to enter the field of protein crystallography. Although much more needs to be done, a well operating crystallization robot has the potential to catalyze the broader adoption of protein crystallography, especially when FedEx-style data collection and increased automation of structure-determination software continue their progress.

To our knowledge, our approach to combine crystallization reagent creation and experiment setup into a single nanovolume robot system is new. Syrrx Inc. has also attempted to create such a system using SynQuad technology. Their robot had 96 dispense heads in a linear array and they provided the reagents as the system fluid, rather than our aspirate and dispense mode. Although technically superior, we feel that our design is more practical, easier to maintain and more compact. Our robot takes up less than 1 $m^2$ of floor space and the entire work area is enclosed in a humidified cabinet (Fig. 2). The aspirate and dispense mode allows us to switch instantly between combinatorial dispensing and pre-made screens and since all dispense units share a single source of system fluid, we can easily prepare a fresh bottle of properly degassed reagent-quality water for this purpose every day. The use of water as a system fluid also allows us to thoroughly flush the entire system with water after each plate setup. Our current focus is to expand the *RoboDrop* program to include special modes for grid, random, incomplete factorial and sparse-matrix screens and to allow users to limit ranges of pH or precipitant concentrations. Most importantly, we need to include a mode where the software automatically generates optimization screens given a set of promising conditions. The current version of the program can be obtained from the authors and is free for academic users.

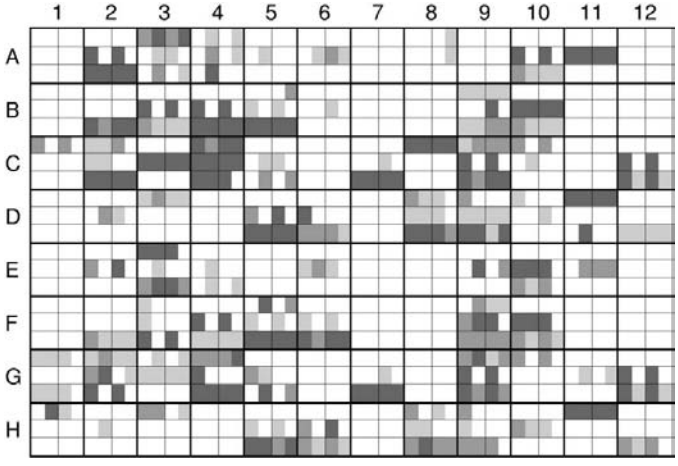


**Figure 5**
Comparison of a commercial screen (Crystal Screen 1 and Crystal Screen 1 Lite; Hampton Research) and the same screen prepared on-the-fly by the robot. The panel represents a 96-well plate in which every well is divided into two colums and three rows. The three rows give results for lysozyme, thaumatin and glucose isomerase, respectively. The left column shows results for the commercial screen and the right column shows the results for the robot-created screen. Within each column the duplicate experiment is represented as two grayscale squares. White, light gray, medium gray and dark gray indicate no crystals, needles or small clusters, small crystals and nice mountable crystals, respectively.

In conclusion, we demonstrate hardware- and software-design features that exploit the inherent flexibility of asynchronous nanovolume non-contact crystallization robots to create crystallization screen solutions and set up the nanovolume crystallization drops with a single instrument. The method does not compromise crystallization-drop quality or speed of screen creation and traditional methods using pre-made screens remain available. Most importantly, our design results in a very compact instrument that requires no complex systems integration and has worked well in our academic facility for over a year.

The authors would like to thank the Alberta Heritage Foundation for Medical Research (AHFMR), the Alberta Science and Research Authority and the Canadian Foundation for Innovation (CFI) for joint funding of the infrastructure. Initial operating funding from CFI and the Alberta Synchrotron Institute is greatly appreciated. The *RoboDrop* logo was created by Maria Elena Vasquez Molina. BH is an AHFMR scholar.

## References

Adams, P. D., Gopal, K., Grosse-Kunstleve, R. W., Hung, L. W., Ioerger, T. R., McCoy, A. J., Moriarty, N. W., Pai, R. K., Read, R. J., Romo, T. D., Sacchettini, J. C., Sauter, N. K., Storoni, L. C. & Terwilliger, T. C. (2004). *J. Synchrotron Rad.* **11**, 53–55.
Blundell, T. L. & Patel, S. (2004). *Curr. Opin. Pharmacol.* **4**, 490–496.
Bott, R. & Boelens, R. (1999). *Curr. Opin. Biotechnol.* **10**, 391–397.
Chayen, N. E. (2003). *J. Struct. Funct. Genomics*, **4**, 115–120.
Chayen, N. E. & Saridakis, E. (2002). *Acta Cryst.* D**58**, 921–927.
Cohen, S. X., Morris, R. J., Fernandez, F. J., Ben Jelloul, M., Kakaris, M., Parthasarathy, V., Lamzin, V. S., Kleywegt, G. J. & Perrakis, A. (2004). *Acta Cryst.* D**60**, 2222–2229.
DeLucas, L. J., Hamrick, D., Cosenza, L., Nagy, L., McCombs, D., Bray, T., Chait, A., Stoops, B., Belgovskiy, A., Wilson, W. W., Parham, M. & Chernov, N. (2005). *Prog. Biophys. Mol. Biol.* **88**, 285–309.
Derewenda, Z. S. (2004). *Structure*, **12**, 529–535.
Dry, S., McCarthy, S. & Harris, T. (2000). *Nature Struct. Biol.* **7**, *Suppl.*, 946–949.
Gaasterland, T. (1998). *Trends Genet.* **14**, 135.
Garman, E. (2003). *Curr. Opin. Struct. Biol.* **13**, 545–551.
Grimm, C., Klebe, G., Ficner, R. & Reuter, K. (2000). *Acta Cryst.* D**56**, 484–488.
Hendrickson, W. A. (2000). *Trends Biochem. Sci.* **25**, 637–643.
Hendrickson, W. A., Horton, J. R. & LeMaster, D. M. (1990). *EMBO J.* **9**, 1665–1672.
Hendrickson, W. A., Horton, J. R., Murthy, H. M., Pahler, A. & Smith, J. L. (1989). *Basic Life Sci.* **51**, 317–324.
Hosfield, D., Palan, J., Hilgers, M., Scheibe, D., McRee, D. E. & Stevens, R. C. (2003). *J. Struct. Biol.* **142**, 207–217.
Jancarik, J. & Kim, S.-H. (1991). *J. Appl. Cryst.* **24**, 409–411.
Krupka, H. I., Rupp, B., Segelke, B. W., Lekin, T. P., Wright, D., Wu, H. C., Todd, P. & Azarani, A. (2002). *Acta Cryst.* D**58**, 1523–1526.
Machius, M. (2003). *Curr. Opin. Nephrol. Hypertens.* **12**, 431–438.
Montelione, G. T., Zheng, D., Huang, Y. J., Gunsalus, K. C. & Szyperski, T. (2000). *Nature Struct. Biol.* **7**, *Suppl.*, 982–985.
Pflugrath, J. W. (2004). *Methods*, **34**, 415–423.
Potterton, E., Briggs, P., Turkenburg, M. & Dodson, E. (2003). *Acta Cryst.* D**59**, 1131–1137.

Rupp, B., Segelke, B. W., Krupka, H. I., Lekin, T., Schafer, J., Zemla, A., Toppani, D., Snell, G. & Earnest, T. (2002). *Acta Cryst.* D**58**, 1514–1518.
Russell, R. B. & Eggleston, D. S. (2000). *Nature Struct. Biol.* **7**, *Suppl.*, 928–930.
Snell, G., Cork, C., Nordmeyer, R., Cornell, E., Meigs, G., Yegian, D., Jaklevic, J., Jin, J., Stevens, R. C. & Earnest, T. (2004). *Structure*, **12**, 537–545.
Stock, D., Perisic, O. & Lowe, J. (2005). *Prog. Biophys. Mol. Biol.* **88**, 311–327.
Sulzenbacher, G. *et al.* (2002). *Acta Cryst.* D**58**, 2109–2115.
Terwilliger, T. C. (2003). *Methods Enzymol.* **374**, 22–37.